Supporting Information

A hydrazono-quinoline-based chemosensor sensing In^{3+} and Zn^{2+} via fluorescence turn-on and ClO^- via color change in aqueous solution

Ahran Kim, Cheal Kim*

Department of Fine Chemistry, Seoul National Univ. of Science & Technology (SNUT), Seoul, 01811, South Korea. Fax: +82-2-972-9149; Tel: +82-2-972-6681; E-mail: chealkim@seoultech.ac.kr

Table S1. Indium chemosensors reported to date.

No.	Sensor	Detection limit (μM)	Percent of water in solution (%)	Method of detection	Reference
1	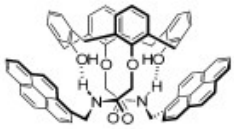	No data	0	**Fluorescence turn-on**	[1]
2	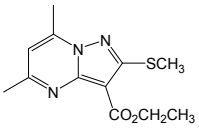	0.19	0	**Fluorescence turn-off**	[2]
3	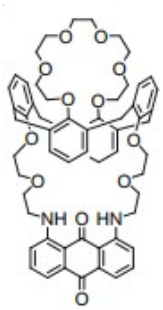	No data	0	**Ratiometric fluorescence change**	[3]
4	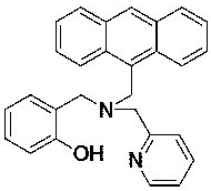	2.0	0	**Fluorescence turn-on**	[4]
5	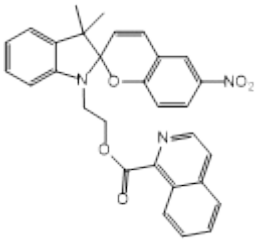	10.0	50	**Fluorescence turn-on Color change**	[5]
6	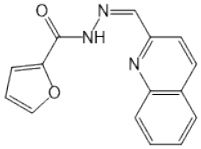	No data	1	**Fluorescence turn-on**	[6]

7	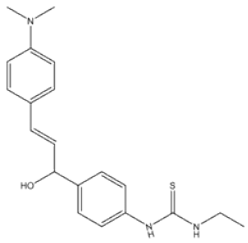	10.4	95	**Fluorescence turn-off Color change**	7
8	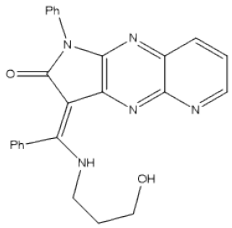	No data	0	**Fluorescence turn-on**	8
9	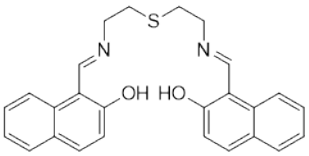	5.89	0	**Fluorescence turn-on**	9
10	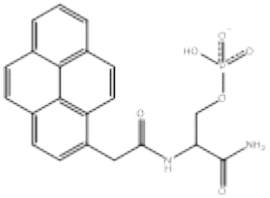	0.064	99	**Ratiometric fluorescence change**	10
11	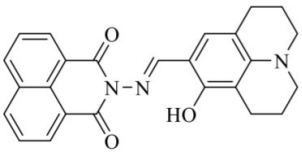	7.92	0	**Fluorescence turn-on**	11
12	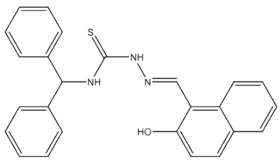	0.89	0	**Fluorescence turn-on**	12
13	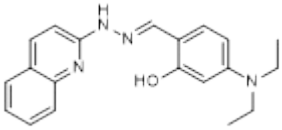	0.05	70	**Fluorescence turn-on**	This work

Reference

1 S. K. Kim, S. H. Kim, H. J. Kim, S. H. Lee, S. W. Lee, J. Ko, R. A. Bartsch and J. S. Kim, *Inorg. Chem.*, 2005, **44**, 7866-7875.

2 Y.-C. Wu, H.-J. Li and H.-Z. Yang, *Org. Biomol. Chem.*, 2010, **8**, 3394–3397.

3 D. Y. Han, J. M. Kim, J. Kim, H. S. Jung, Y. H. Lee, J. F. Zhang and J. S. Kim, *Tetrahedron Lett.*, 2010, **51**, 1947–1951.

4 H. Kim, K. B. Kim, E. J. Song, I. H. Hwang, J. Y. Noh, P. G. Kim, K. D. Jeong and C. Kim, *Inorg. Chem. Commun.*, 2013, **36**, 72–76.

5 Y.-M. Kho and E. Shin, *Molecules*, 2017, **22**, 1569.

6 A. Kim, J. H. Kang, H. J. Jang and C. Kim, *J. Ind. Eng. Chem.*, 2018, **65**, 290-299.

7 M. Lo Presti, S. El Sayed, R. Martínez-Máñez, A. M. Costero, S. Gil, M. Parra and F. Sancenón, *New J. Chem.*, 2016, **40**, 9042–9045.

8 K. Ostrowska, A. Kaźmierska, M. Rąpała-Kozik and J. Kalinowska-Tłuścik, *New J. Chem.*, 2014, **38**, 213–226.

9 S. Y. Lee, M. Yang and C. Kim, *Spectrochim. Acta A*, 2018, **205**, 622–629.

10 P. K. Mehta, G. W. Hwang, J. Park and K.-H. Lee, *Anal. Chem.*, 2018, **90**, 11256–11264.

11 H. J. Jang, J. H. Kang, D. Yun and C. Kim, *Photochem. Photobiol. Sci.*, 2018, **17**, 1247–1255.

12 C. Kim and J. B. Chae, *J. Fluoresc*, 2018, **28**, 1363–1370.

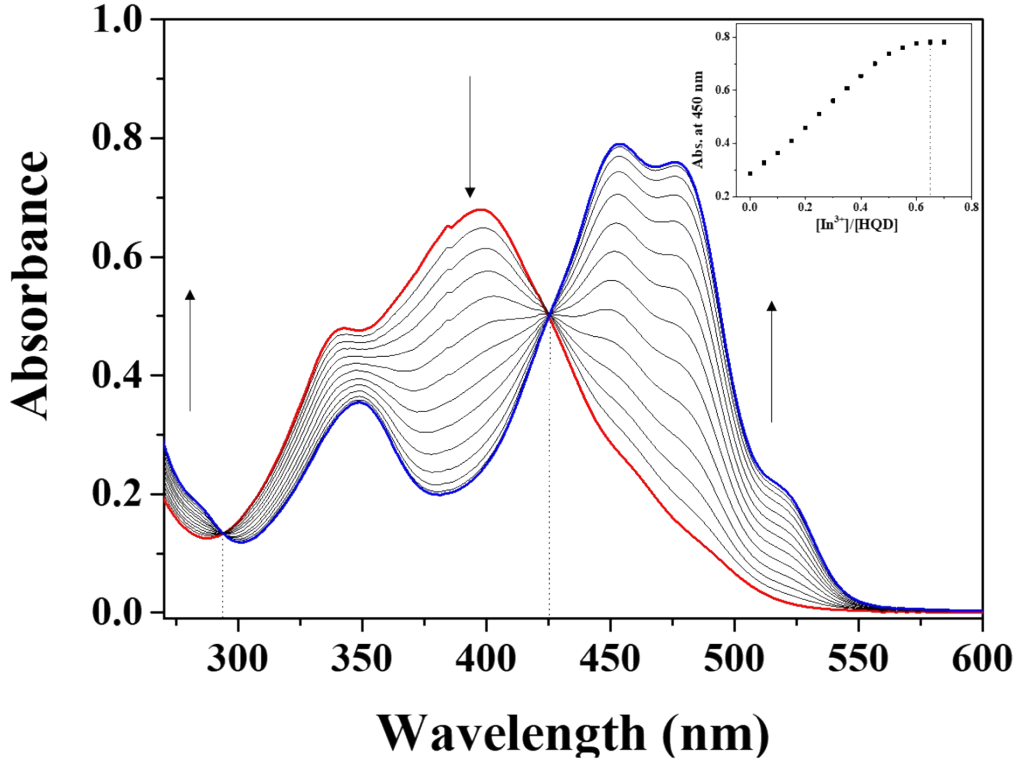

Fig. S1 Change of UV-vis spectra of **HQD** (30 μM) with different indium concentration.

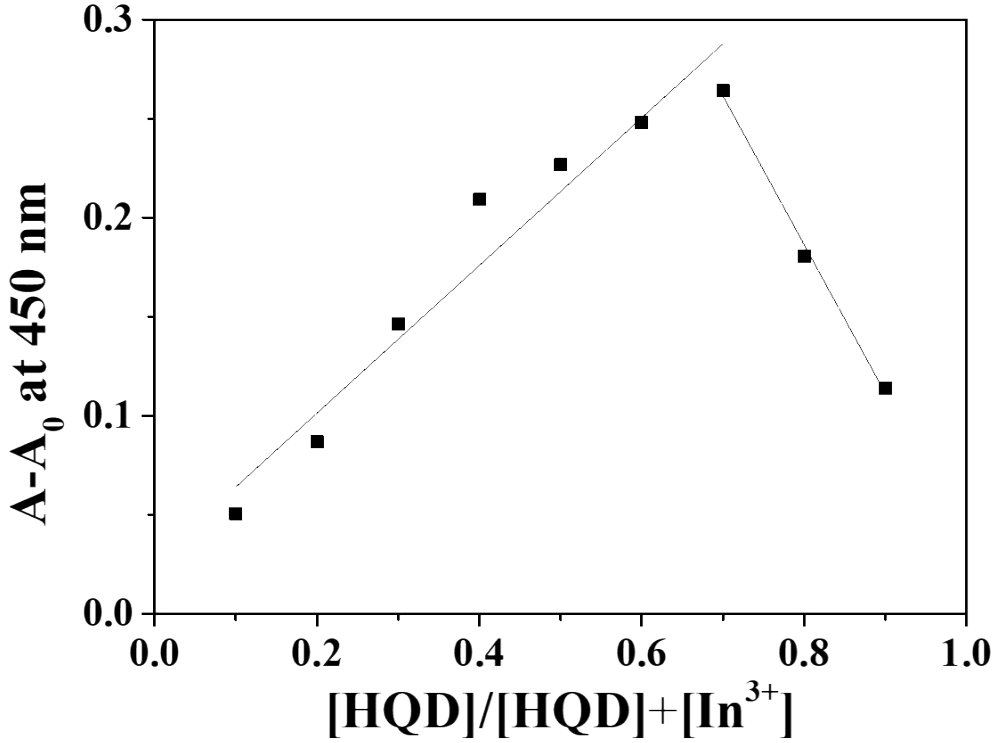

Fig. S2 Job plot of **HQD** with In^{3+}. Absorbance at 450 nm was plotted as a function of the molar ratio of [**HQD**]/([**HQD**]+[In^{3+}]). The total concentration of In^{3+} with sensor **HQD** was 30 μM. [A is the absorbance of **HQD**-In^{3+} and A_0 is the absorbance of **HQD**].

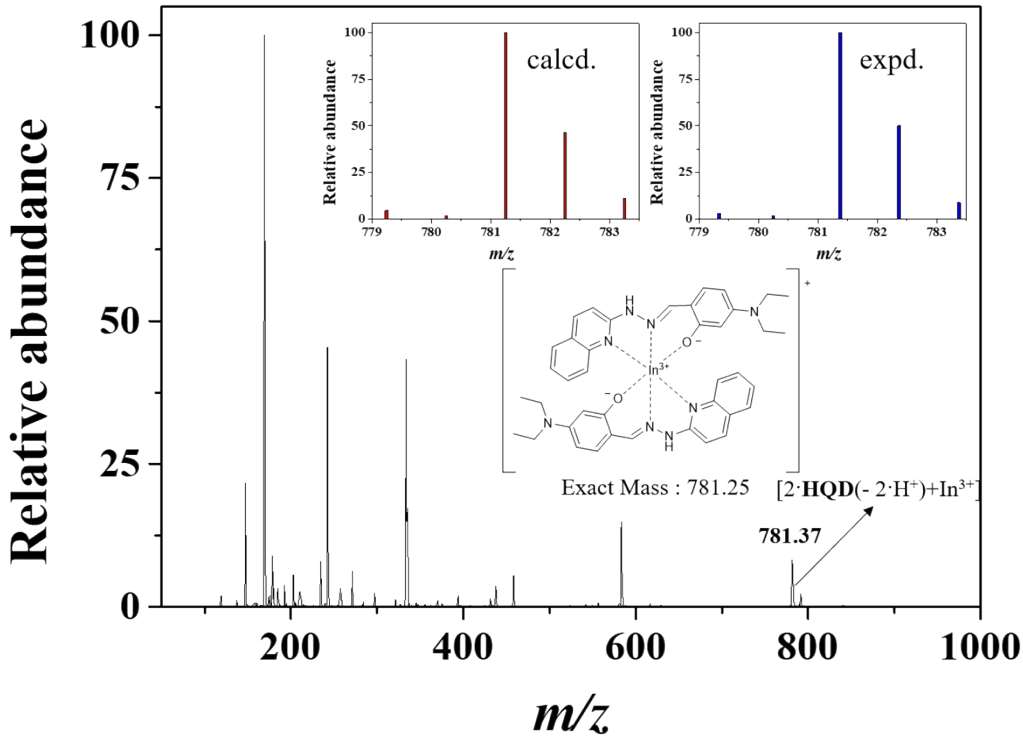

Fig. S3 Positive-ion electrospray ionization (ESI) mass spectrum and pattern of sensor **HQD** (100 μM) upon addition of indium ion (50 μM).

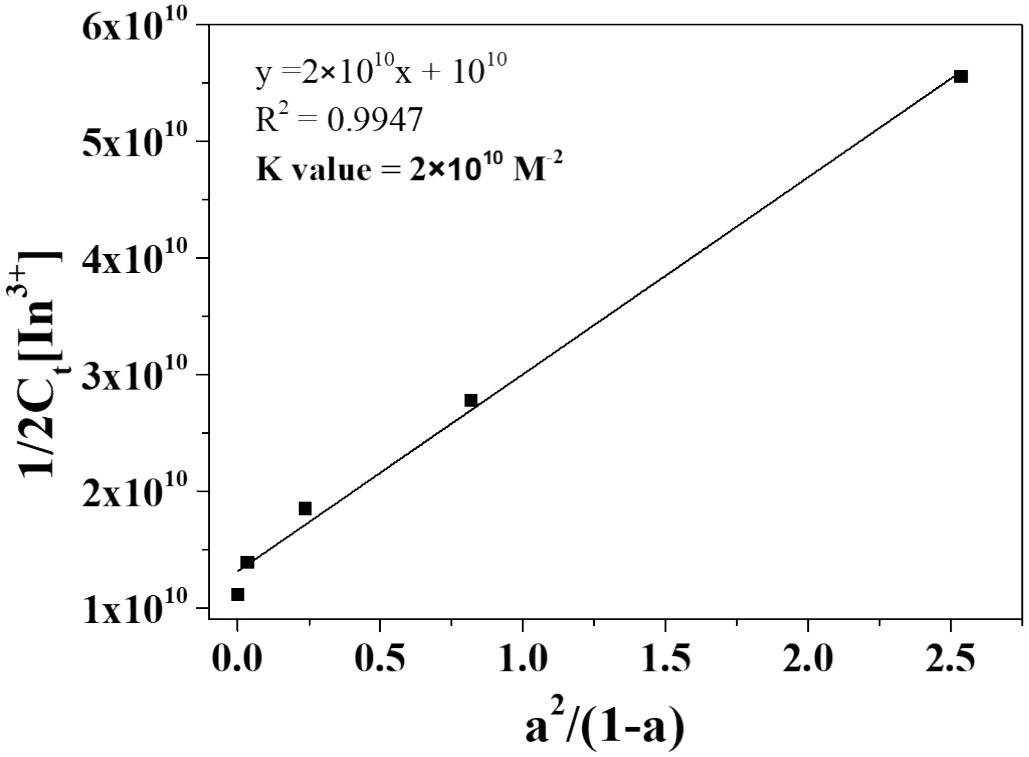

Fig. S4 Li's equation plot of **HQD** (30 μM) for In^{3+}.

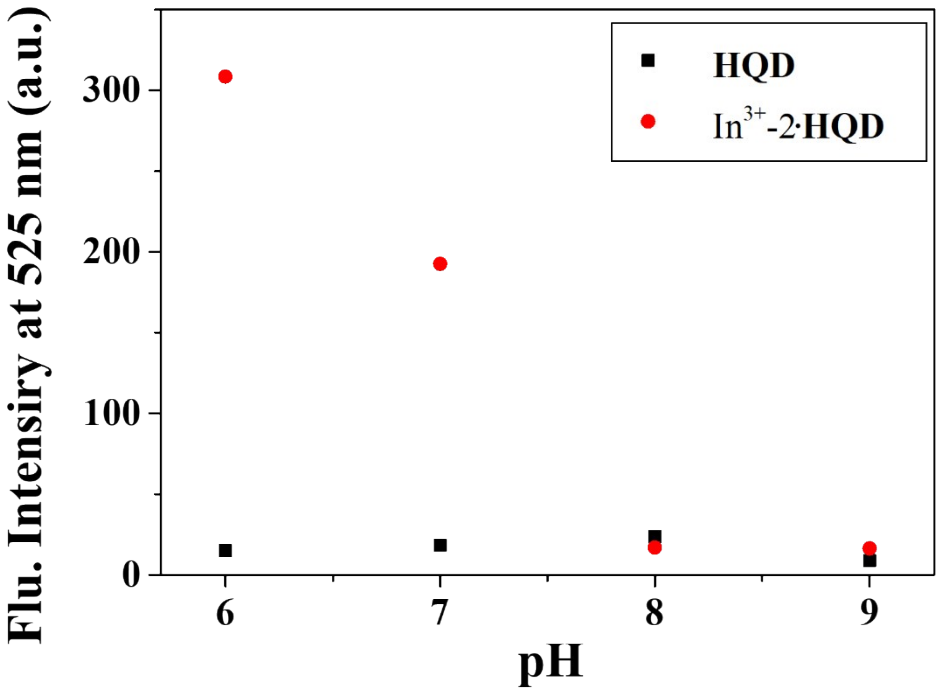

Fig. S5 Fluorescence intensity (525nm) of **HQD** and In^{3+}-2· **HQD** in different pH.

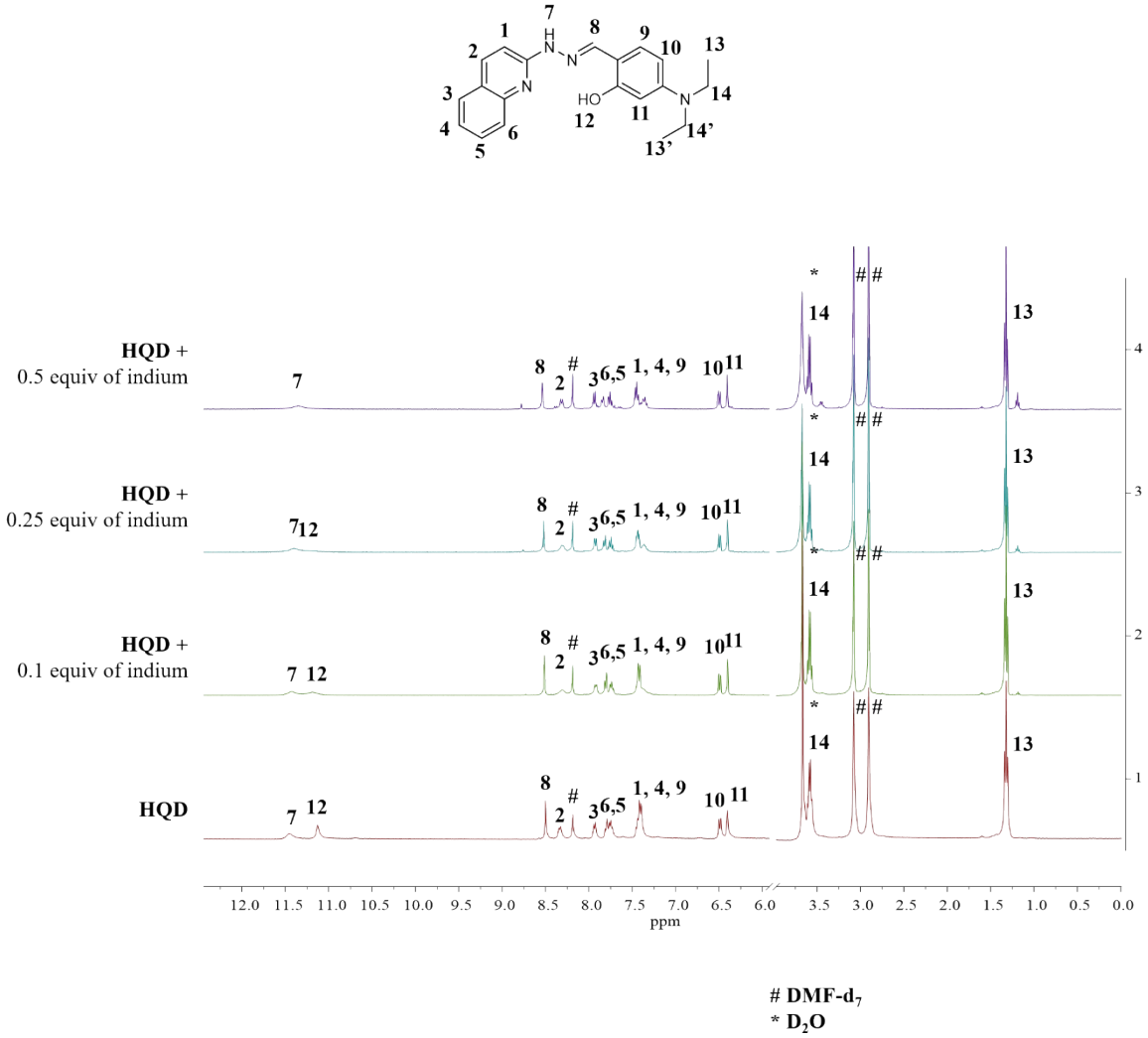

Fig. S6 ^{1}H NMR titration of **HQD** with $In(NO_3)_3$.

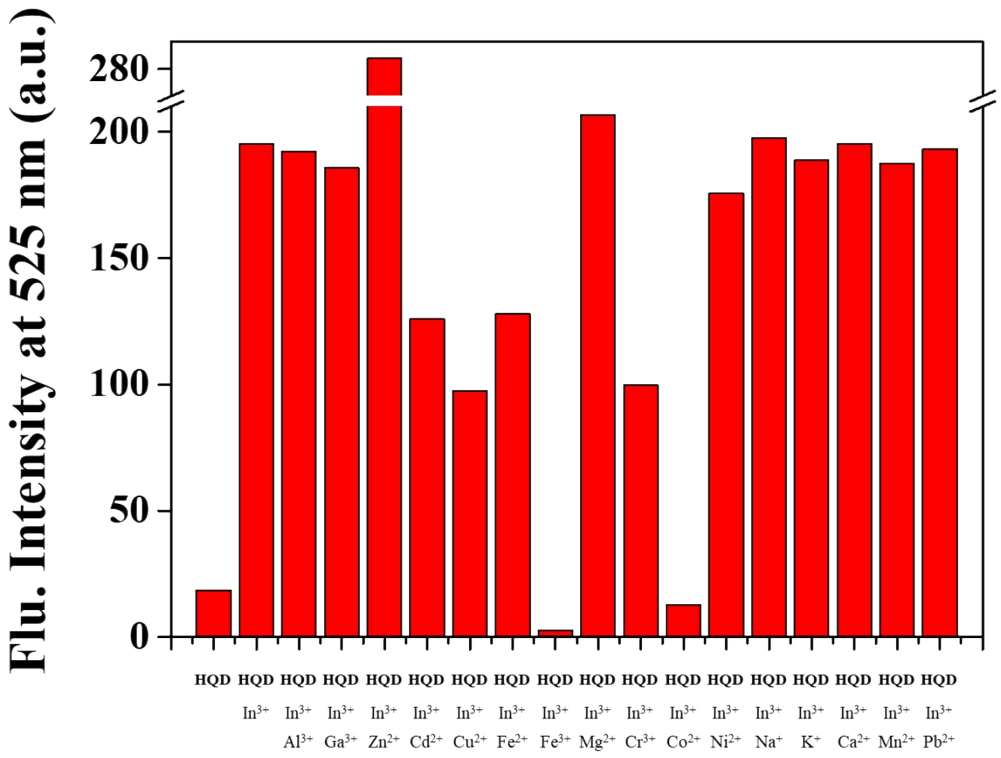

Fig. S7 Competitive selectivity of **HQD** (30 μM) toward In^{3+} ions (0.5 equiv) in the presence of other metal ions (0.5 equiv).

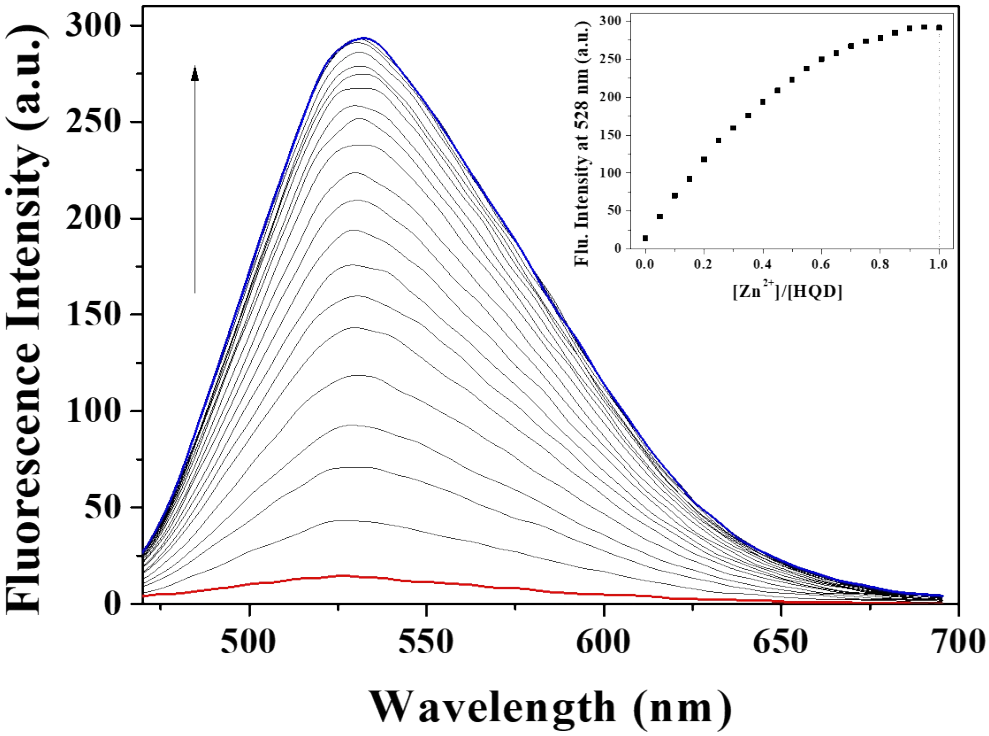

Fig. S8 Change of fluorescence spectra of **HQD** (30 μM) with different Zn^{2+} concentration.

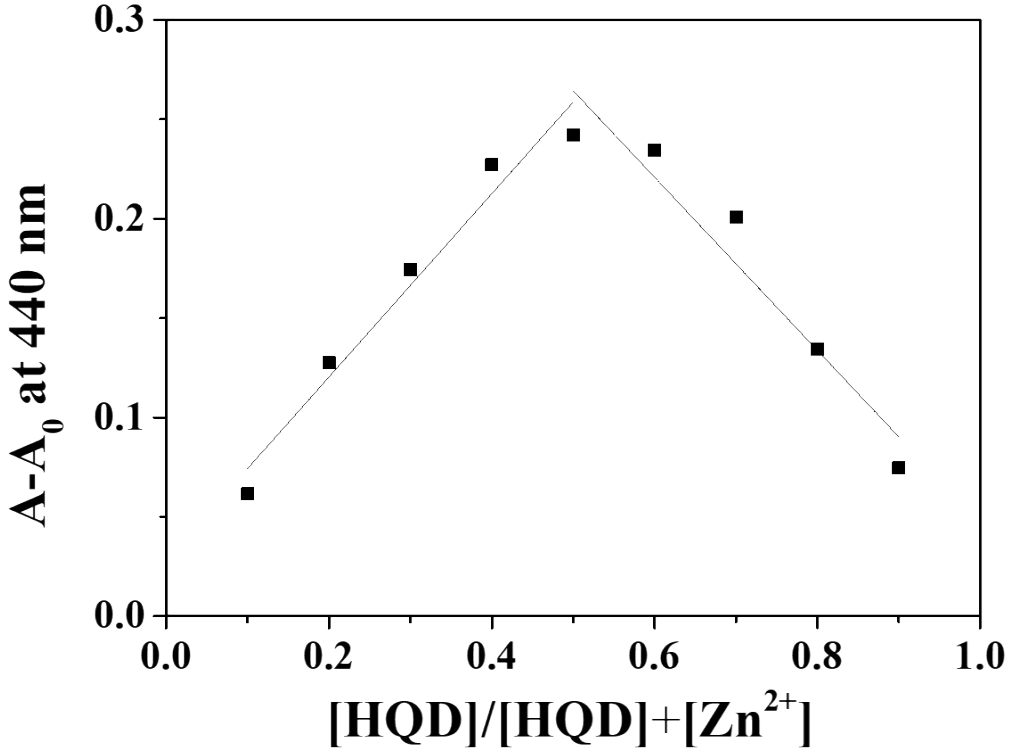

Fig. S9 Job plot of **HQD** with Zn^{2+}. Absorbance at 440 nm was plotted as a function of the molar ratio of [**HQD**]/([**HQD**]+[Zn^{2+}]). The total concentration of Zn^{2+} ions with sensor **HQD** was 30 μM. [A is the absorbance of **HQD**-Zn^{2+} and A_0 is the absorbance of **HQD**].

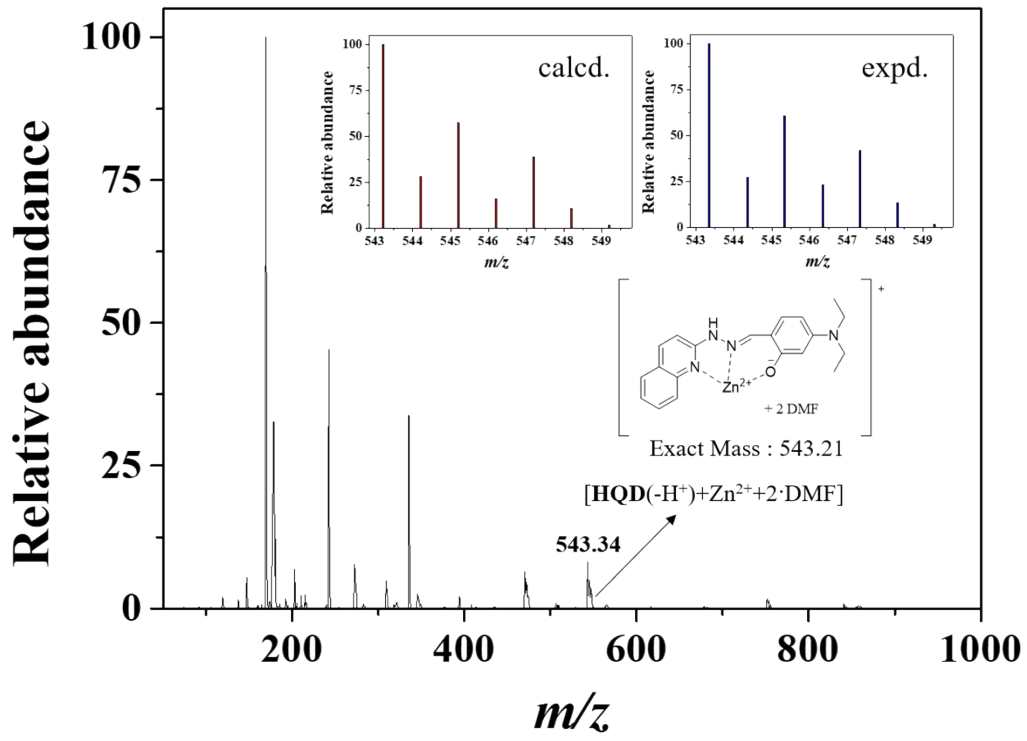

Fig. S10 Positive-ion electrospray ionization (ESI) mass spectrum of **HQD** (100 μM) upon addition of zinc ion (1 equiv).

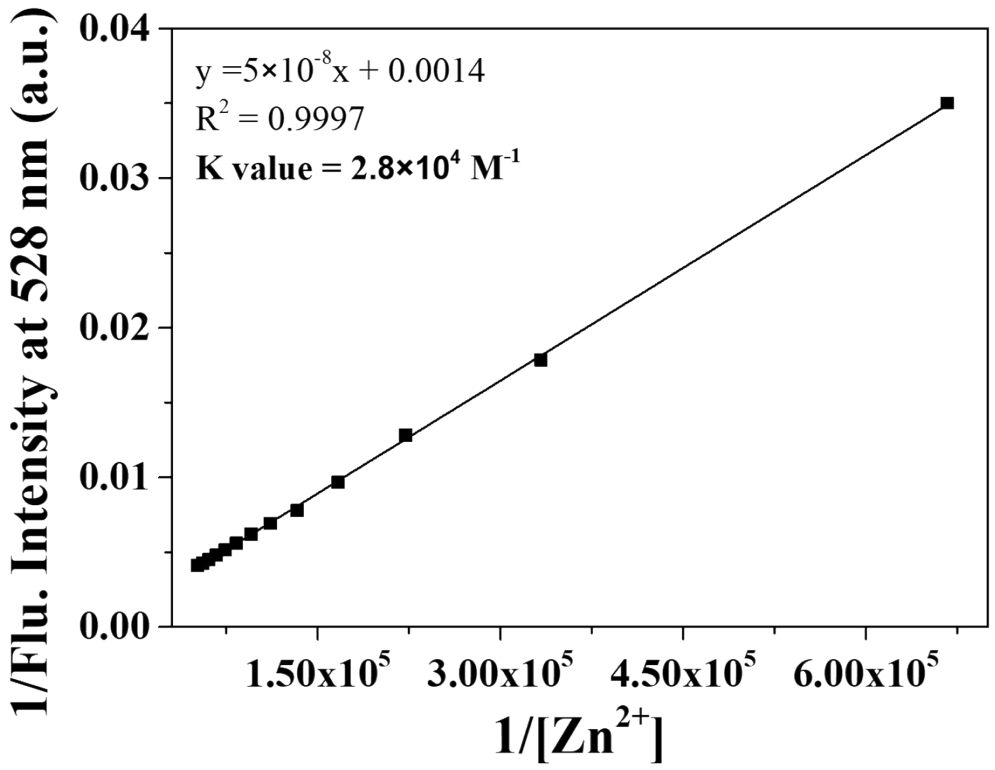

Fig. S11 Benesi-Hildebrand equation plot of **HQD** (30 μM) for Zn^{2+}.

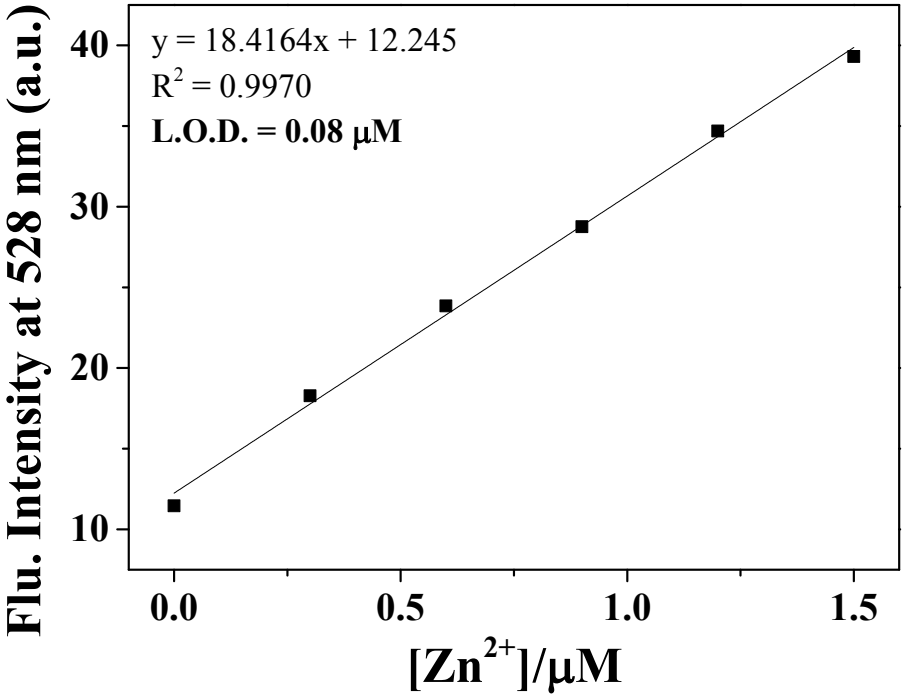

Fig. S12 L.O.D. for Zn^{2+} by **HQD** (30 μM) based on the 3σ/slope.

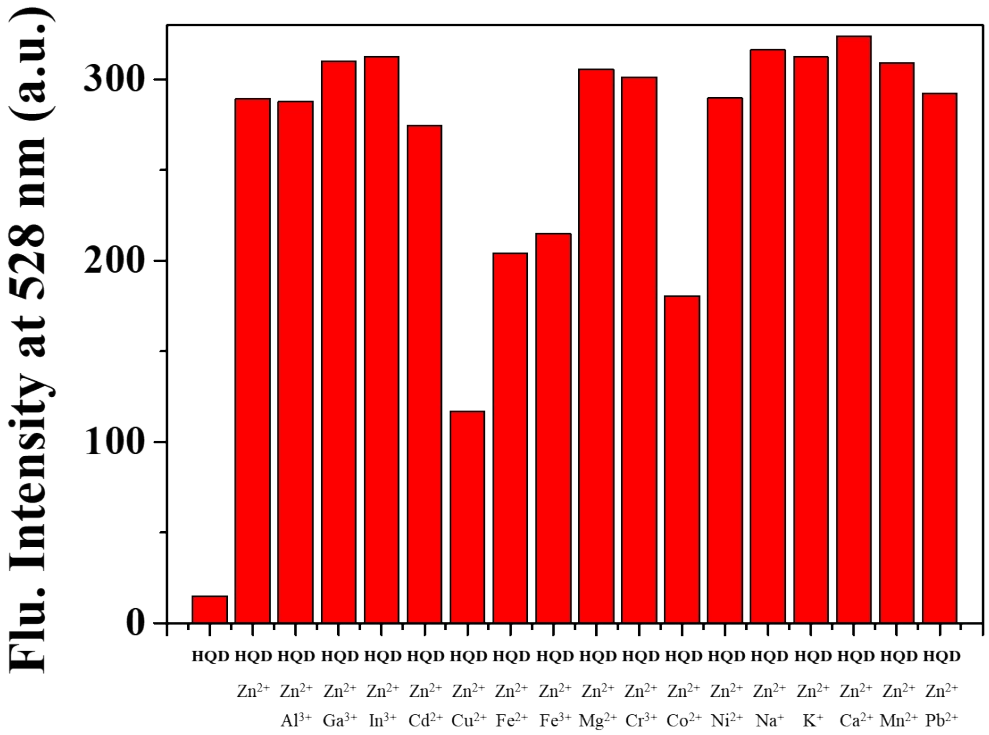

Fig. S13 Competitive selectivity of **HQD** (30 μM) toward Zn^{2+} ions (1 equiv) in the presence of other metal ions (1 equiv).

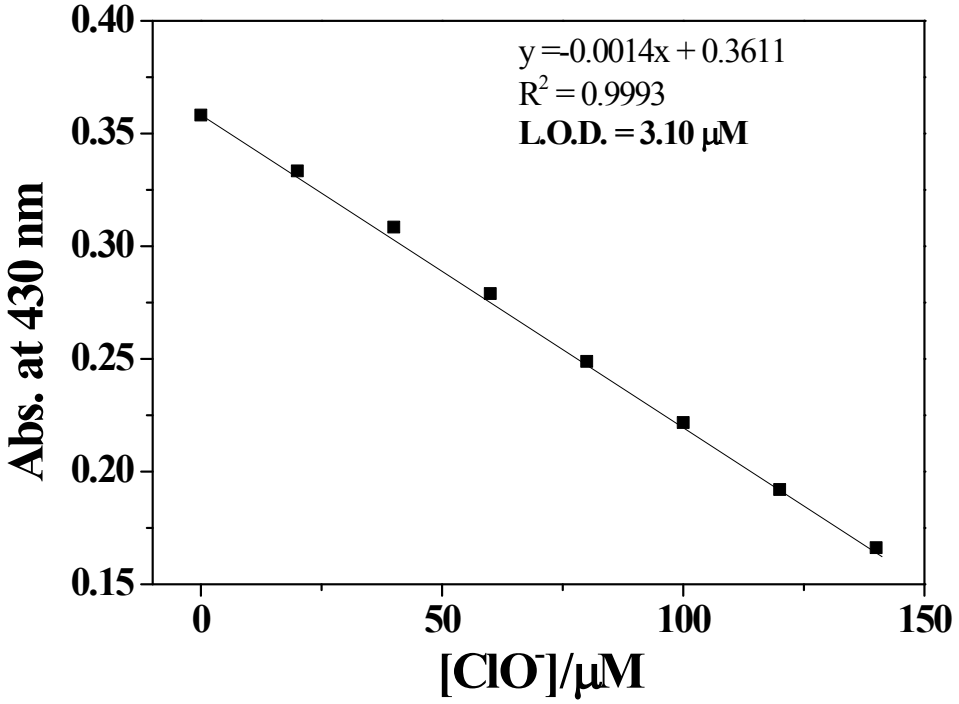

Fig. S14 L.O.D. for ClO^- by **HQD** (20 μM) based on the 3σ/slope.

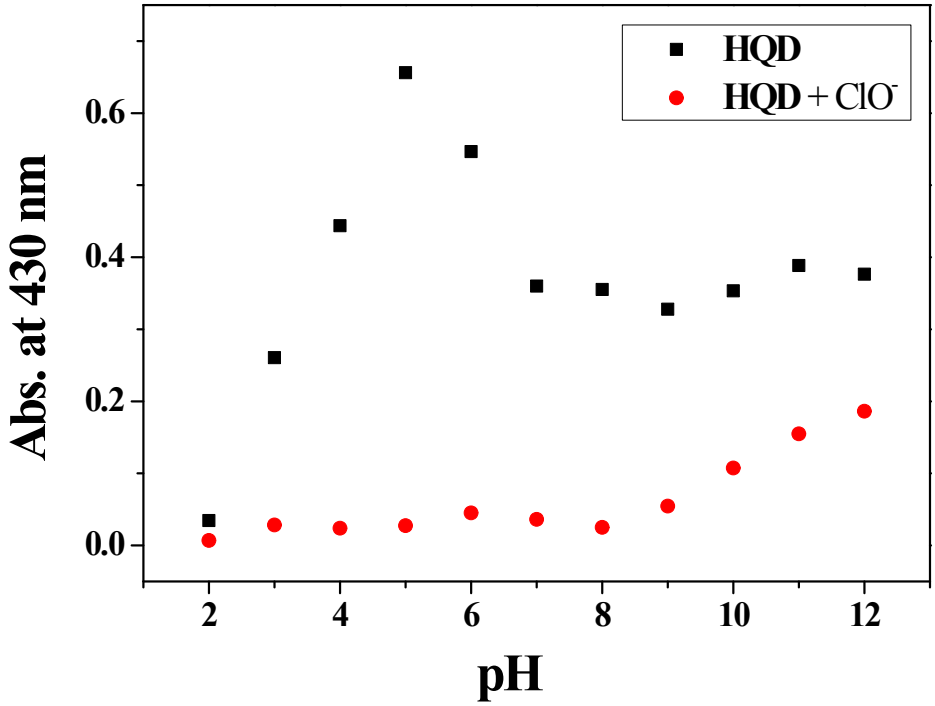

Fig. S15 Absorbance (430 nm) of **HQD** and **HQD** with ClO^- in different pH.

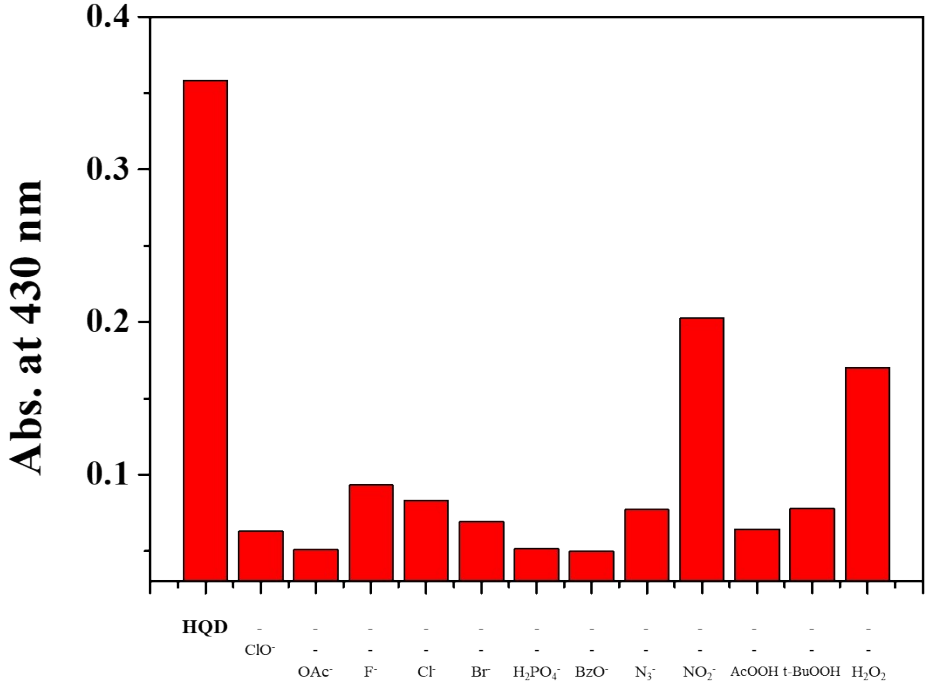

Fig. S16 Abosrbance (430 nm) of **HQD** (20 μM) toward ClO^- (20 equiv) in the presence of other anions and ROS (20 equiv).

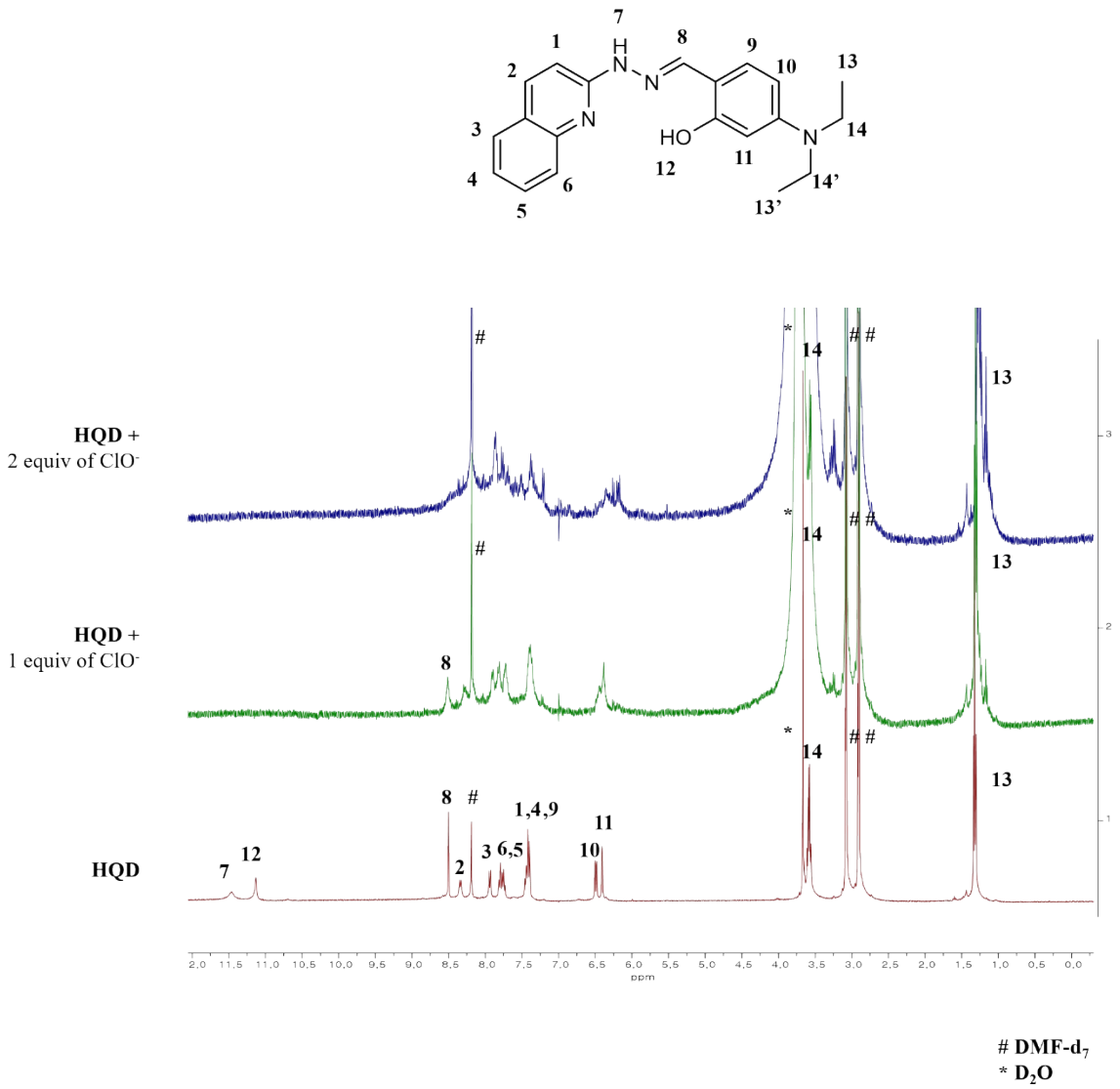

Fig. S17 ^{1}H NMR titration of **HQD** with NaClO.

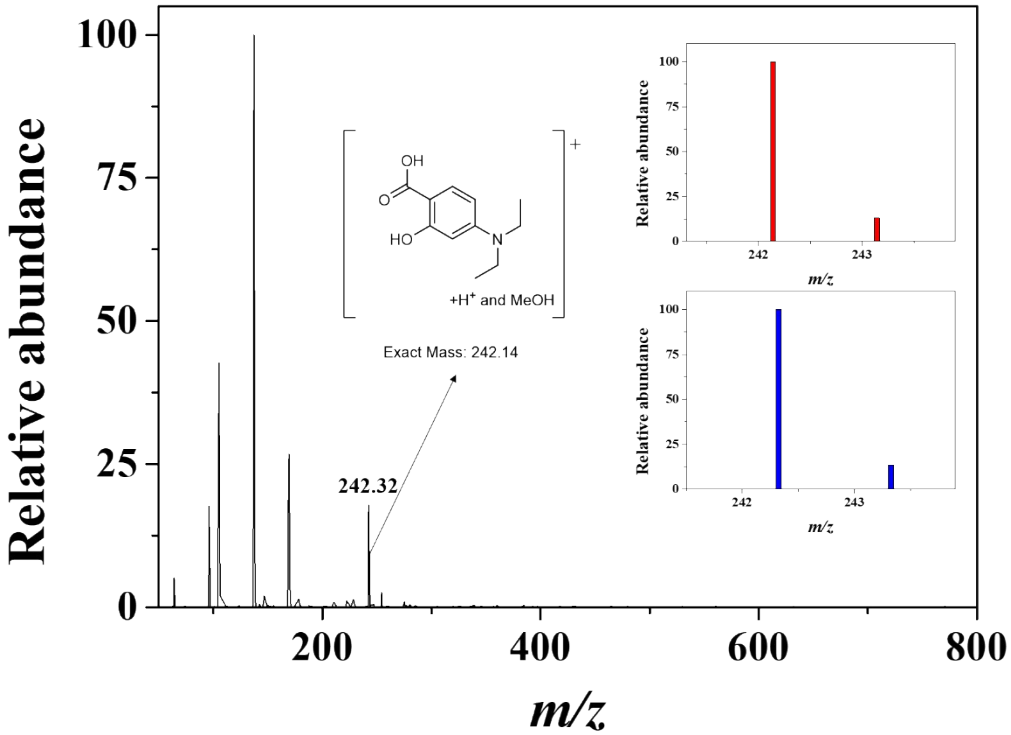

Fig. S18 Positive-ion electrospray ionization (ESI) mass spectrum and pattern of sensor **HQD** (100 μM) upon addition of NaClO (1 equiv).

(a)

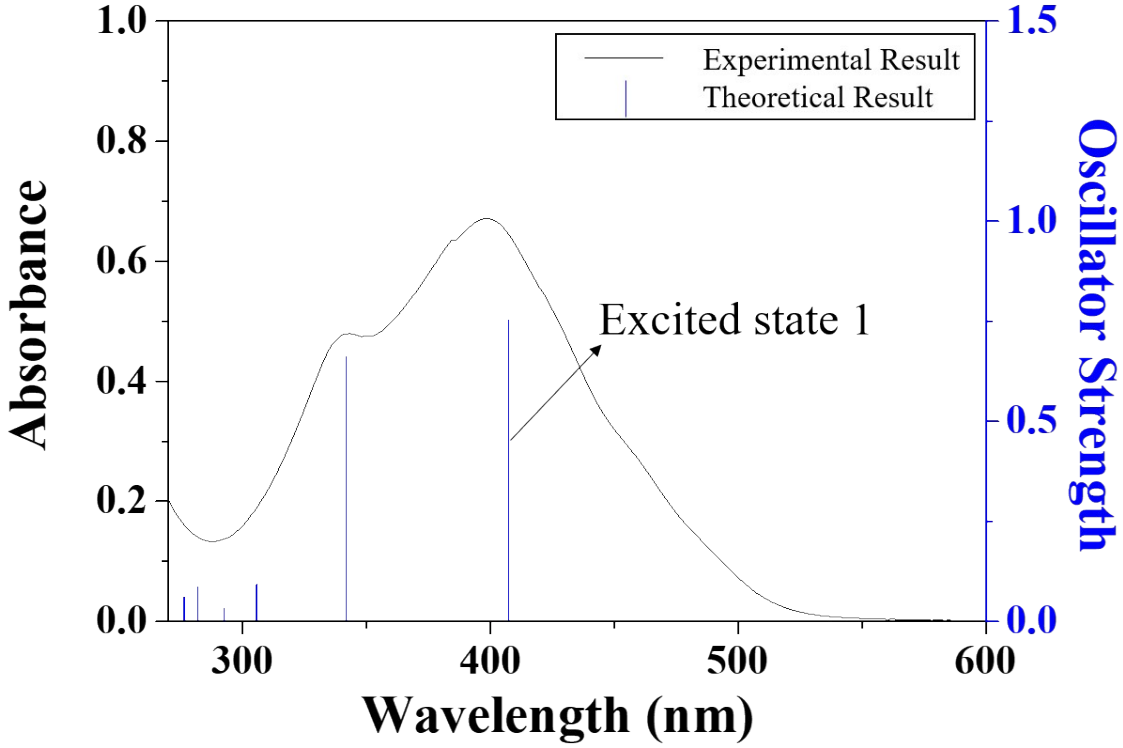

(b)

Excited state 1	Wavelength (nm)	Percent (%)	Main Character	Oscillator strength
H ⟶ L	407.41	99	ICT	0.7541

Fig. S19 (a) The theoretical excitation energies and the experimental UV-vis spectrum of **HQD**. (b) The major electronic transition energies and molecular orbital contributions of **HQD** (H = HOMO and L = LUMO).

(a)

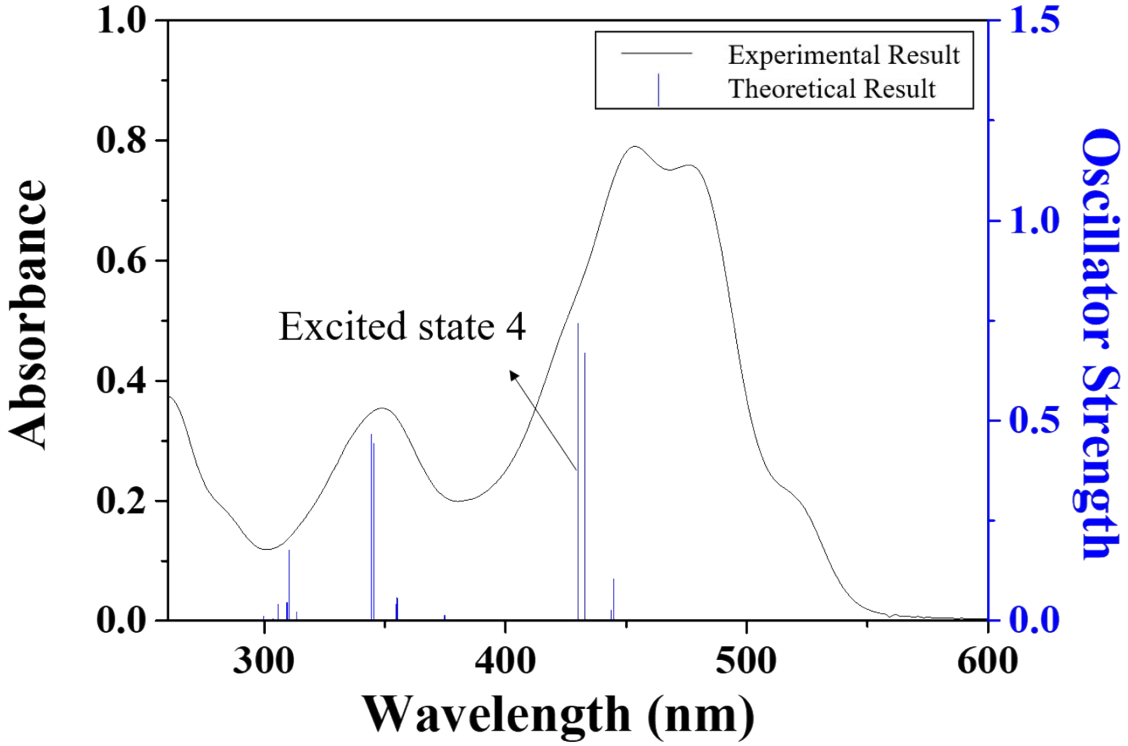

(b)

Excited state 4	Wavelength (nm)	Percent (%)	Main Character	Oscillator strength
H ⟶ L+1	430.18	67	ICT	0.7444
H-1 ⟶ L		31	ICT	

Fig. S20 (a) The theoretical excitation energies and the experimental UV-vis spectrum of In^{3+}-2·**HQD**. (b) The major electronic transition energies and molecular orbital contributions of In^{3+}-2·**HQD** (H = HOMO and L = LUMO).

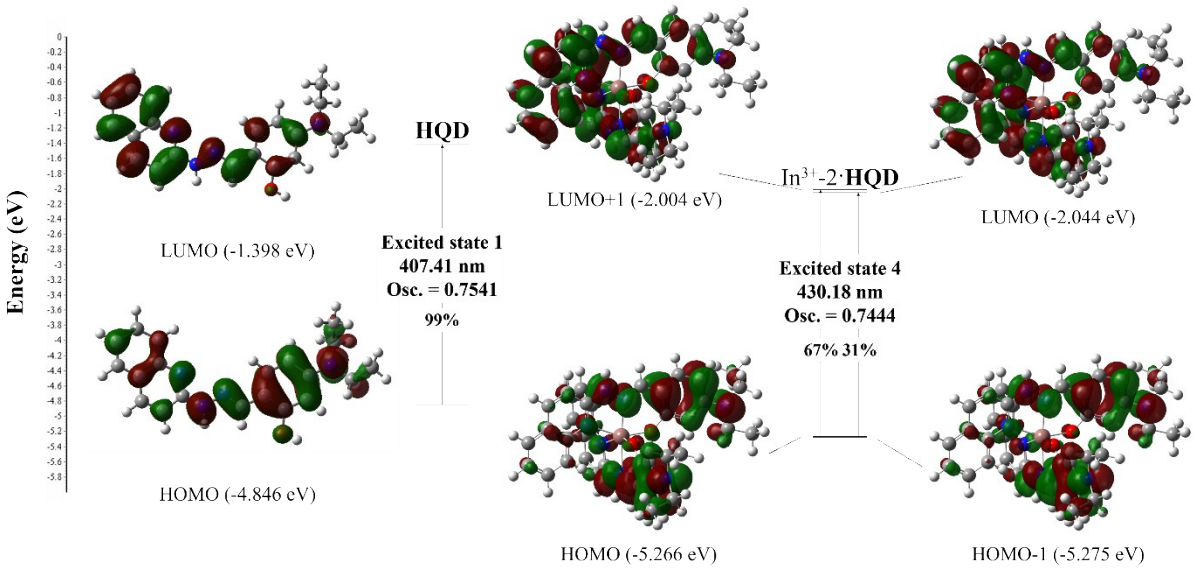

Fig. S21 The major molecular orbital transitions and excitation energies of **HQD** and its In^{3+} complex.

(a)

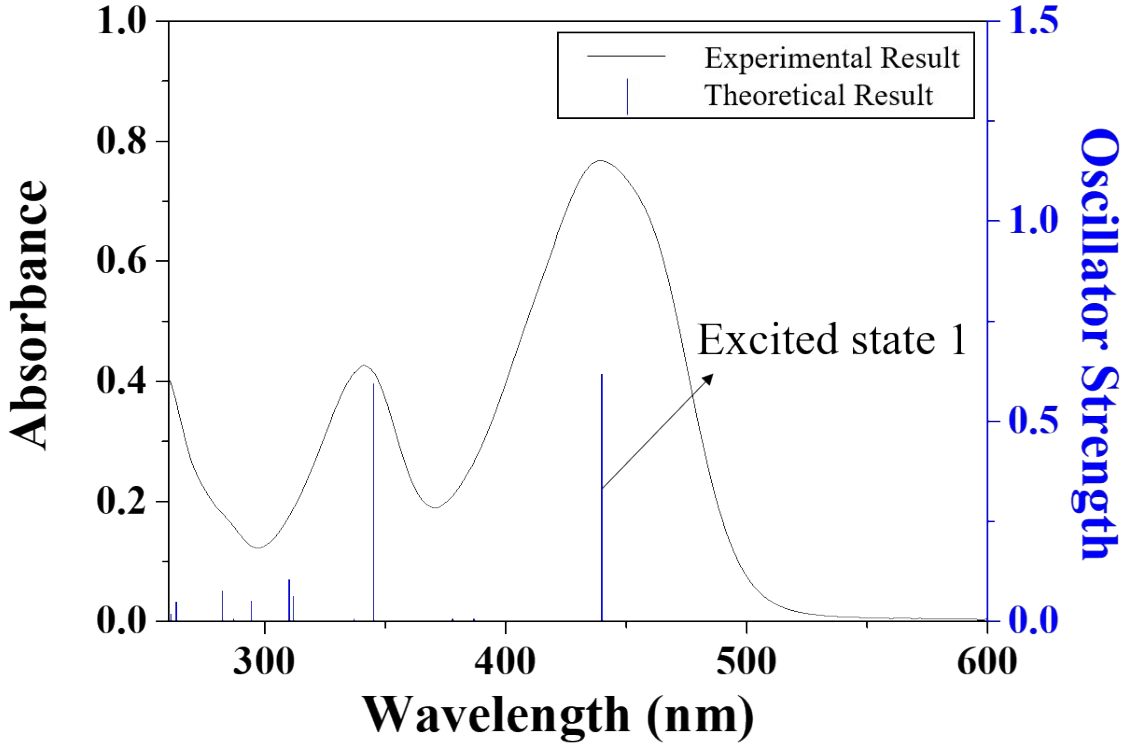

(b)

Excited state 1	Wavelength (nm)	Percent (%)	Main Character	Oscillator strength
H ⟶ L	439.78	98	ICT	0.6175

Fig. S22 (a) The theoretical excitation energies and the experimental UV-vis spectrum of **HQD**-Zn^{2+} complex. (b) The major electronic transition energies and molecular orbital contributions of **HQD**-Zn^{2+} complex (H = HOMO and L = LUMO).

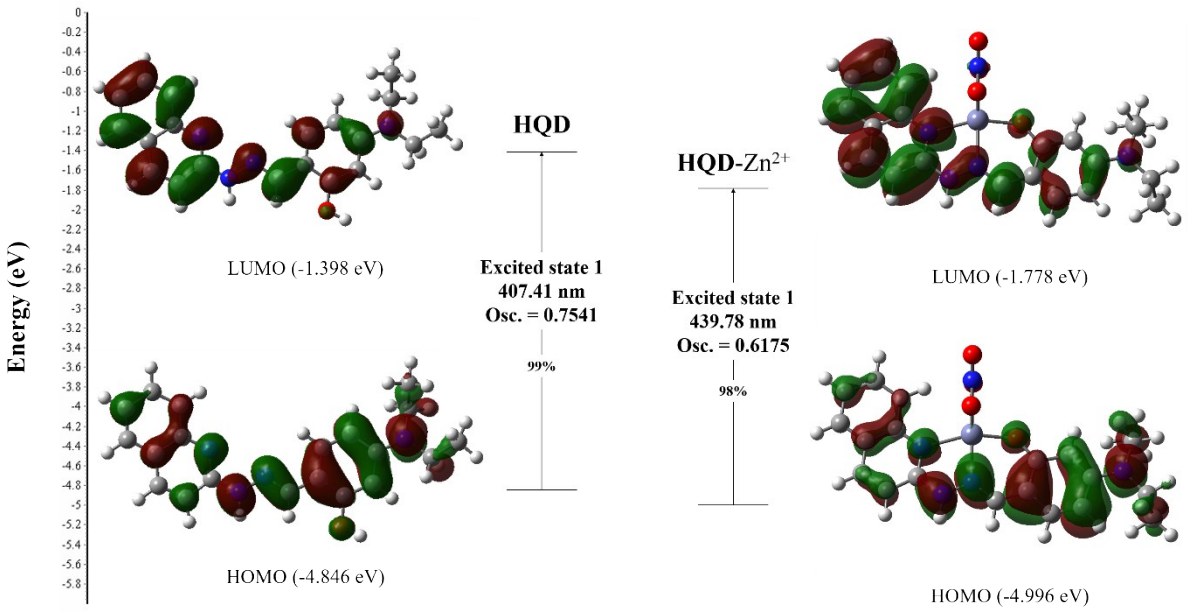

Fig. S23 The major molecular orbital transitions and excitation energies of **HQD** and its Zn^{2+} complex.

(a)

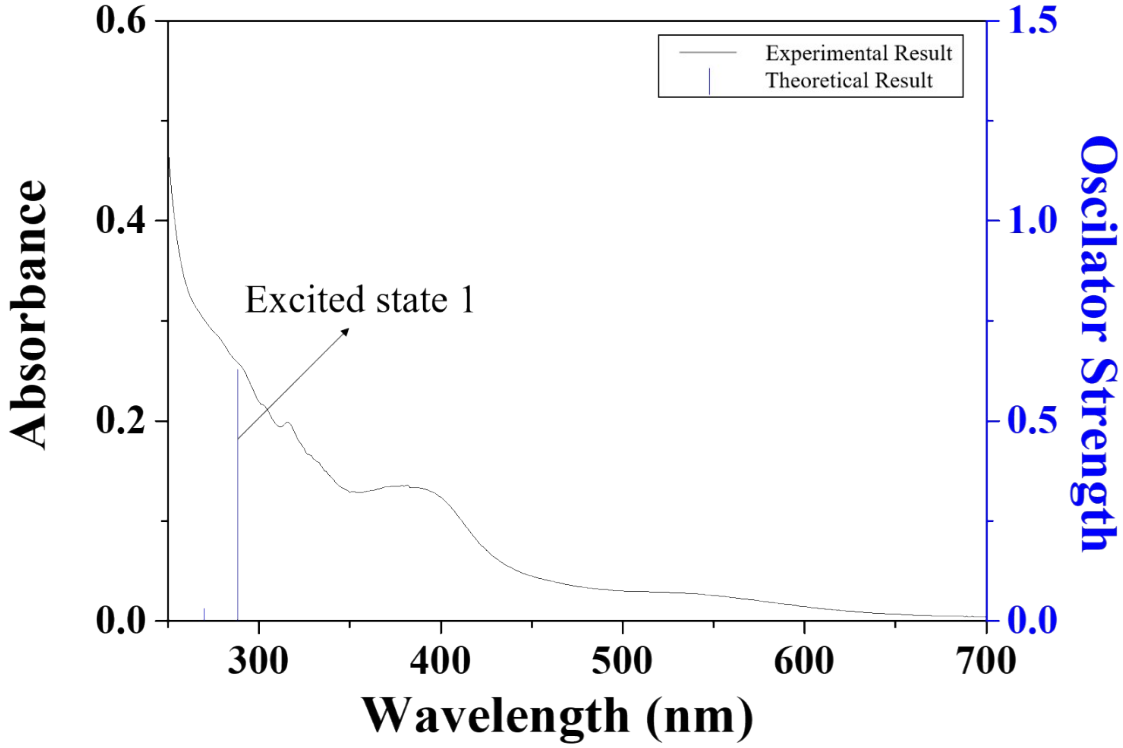

(b)

Excited state 1	Wavelength (nm)	Percent (%)	Main Character	Oscillator strength
H ⟶ L	288.21	95	ICT	0.6298

Fig. S24 (a) The theoretical excitation energies and the experimental UV-vis spectrum of **DCA**. (b) The major electronic transition energies and molecular orbital contributions of **DCA** (H = HOMO and L = LUMO).

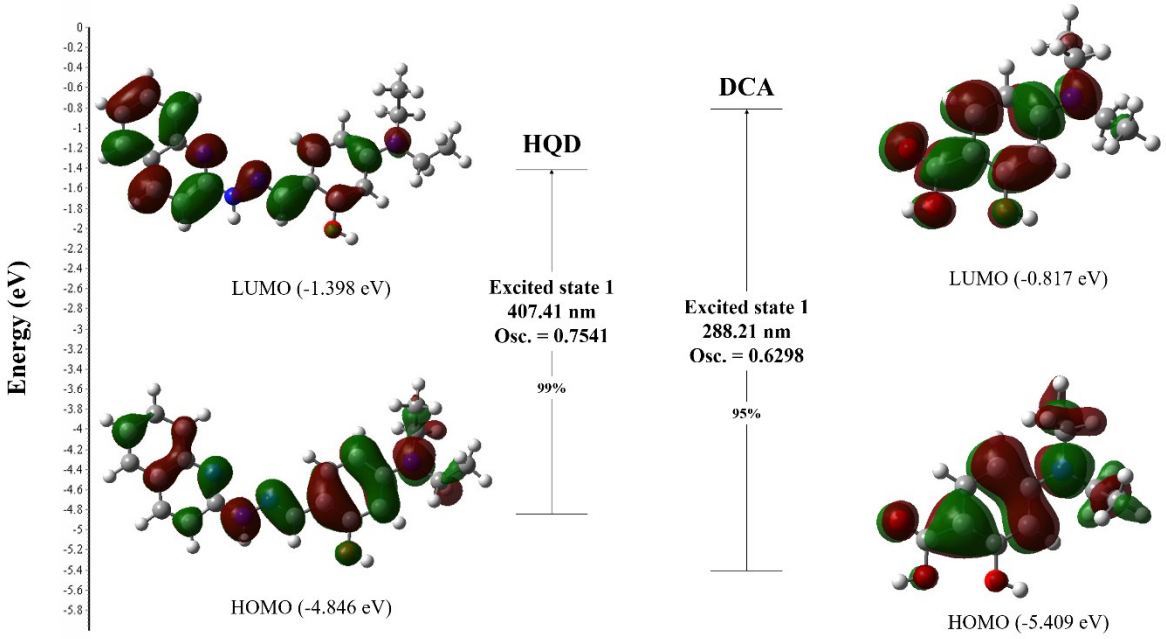

Fig. S25 The major molecular orbital transitions and excitation energies of **HQD** and **DCA**.